Hindawi
Journal of Nanomaterials
Volume 2017, Article ID 9621515, 8 pages
https://doi.org/10.1155/2017/9621515

Research Article

Facile Preparation of Porous Inorganic SiO_2 Nanofibrous Membrane by Electrospinning Method

Meng-Jie Chang, Wen-Na Cui, and Jun Liu

Department of Materials Science and Engineering, Xi'an University of Science and Technology, Xi'an 710054, China

Correspondence should be addressed to Jun Liu; jun_liu@xust.edu.cn

Received 8 August 2017; Revised 23 November 2017; Accepted 5 December 2017; Published 24 December 2017

Academic Editor: Yoke K. Yap

We presented a straightforward method to fabricate porous inorganic SiO_2 nanofibrous membrane by one-step calcination of electrospun nanofibers, which encapsulated with carbon nanospheres as template for nanopore generation. The structure, morphology, and composition of the as-spun fibers (PVA/SiO_2/C) and porous SiO_2 were characterized by Fourier transform infrared spectroscopy (FTIR), X-ray diffraction (XRD), transmission electron microscopy (TEM), and scanning electron microscopy (SEM). The detective results indicated that the carbon nanospheres were uniformly encapsulated inside the PVA/SiO_2/C nanofibers. After calcination, PVA polymer was removed and high flexible inorganic nanofibrous membrane composed of amorphous SiO_2 was obtained. Simultaneously, carbon nanosphere template was decomposed and uniform nanopores were generated inside the SiO_2 nanofibers. This new method is simple and of low cost and hence is suitable to prepare other porous inorganic nanofibers with high surface area for practical application.

1. Introduction

Electrospinning is a simple and versatile technique capable of generating ultrafine continuous fibers from a variety of materials [1–5]. Electrospun fibrous membranes possess several fascinating features that make them very attractive for separation and adsorption of contaminants, such as a large surface-to-volume ratio, high porosity, interconnected open pore structure, and high permeability [6–9]. In particular, porous electrospun nanofibers have been proposed to enhance the performance with higher absorbance capacity and separation efficiency [10]. To this purpose, several methods based on phase separation and template sacrifice have been developed for the preparation of porous nanofibers [11–14]. For example, Wu et al. reported superhydrophobic and superoleophilic polystyrene fibrous sorbent films by controlling the vapor-induced phase separation [15]; McCann and coworkers fabricated highly porous titania nanofibers by calcining fibers from coaxial electrospinning technology [16]. Moreover, Lee and colleagues produced macroporous carbon fibers with macroscopic surface openings by carbonization of polymethyl methacrylate (PMMA) colloid incorporated polyacrylonitrile (PAN) fibers [17]. Recently, we fabricated nanoporous poly(vinyl alcohol) (PVA) nanofibers by removal of Fe_3O_4 particle template and cross-link of PVA fibers simultaneously [18]. However, the above porous fibers are still limited for wide application because of the following several shortages. First, the obtained organic fibers suffer from the chemical and thermal stability. Second, routine inorganic materials are usually fragile to break into segments, which makes it difficult to achieve separation and recycle conveniently. Therefore, development of flexible porous inorganic membranes is of great interest for practical applications.

Inorganic SiO_2 nanofibrous membrane has both flexible and high-heat-resistant properties, which can be fabricated by a combination of electrospinning with sol-gel process, followed by calcination [19, 20]. Previously, hollow SiO_2 nanofibers have been prepared by controlling the ratios of H_2O/C_2H_5OH or TEOS/PVP in the precursor solution [21, 22]. The above methods show feasibility to produce hollow fibers based on phase separation process; however, it is still a challenge to produce porous silica nanofibers. To the best of our knowledge, there are few reports on porous SiO_2 nanofibers.

In this work, we present a novel method to fabricate porous inorganic SiO_2 nanofibrous membranes by electrospinning using carbon nanosphere as templates. The carbon nanospheres were first synthesized by hydrothermal method and then mixed with silica sol-gel as precursor solution. The porous SiO_2 nanofibrous membrane was directly fabricated by electrospinning and postcalcinations. After calcinations, spherical nanopores were left at the position where carbon nanosphere templates were located. Importantly, polycondensation of SiO_2 and decomposition of carbon nanosphere and PVA can be accomplished in one step during the calcination, simplifying the operation and saving time to form porous SiO_2 nanofibers.

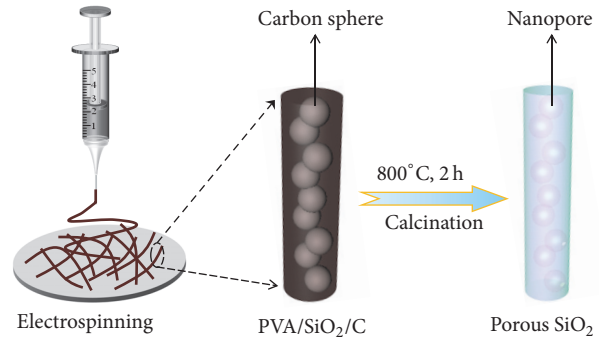

Figure 1: Scheme for fabricating porous SiO_2 fibers via electrospinning and calcinations.

2. Experimental Section

Polyvinyl alcohol (PVA, 87–89% hydrolyzed, molecular weight 88,000–97,000) was purchased from Alfa Aesar Inc. Tetraethyl orthosilicate (TEOS), phosphoric acid (85 wt%), and glucose were received from Guoyao Inc. The high voltage supply for electrospinning was purchased from Dongwen (Tianjing).

2.1. Synthesis of Carbon Nanospheres. Carbon nanospheres were synthesized by using hydrothermal method as described elsewhere [23]. Briefly, 8 g of glucose was dissolved in 40 mL of deionized (DI) water to form a transparent solution, which was then transferred into a Teflon-lined autoclave (50 mL) and sealed. The autoclave was maintained at 180°C for 5 h in an electrical oven. After naturally cooling down to room temperature, the carbon nanospheres were isolated and rinsed by centrifugation at 12000 rpm/min for 15 min for several cycles with DI water and then dried at 60°C.

2.2. Fabrication of Porous SiO_2 Nanofibers. Porous SiO_2 nanofibers were fabricated by electrospinning and postcalcinations. TEOS was used as an alkoxide precursor of SiO_2 while PVA served as both a carrying polymer for TEOS and a precursor of PVA nanofiber. A PVA solution (11 wt%) was prepared by dissolving PVA powders in DI water at 80°C with vigorous stirring. A silica gel was prepared by hydrolysis and polycondensation of TEOS assisted by the dropwise addition of H_3PO_4 with stirring at room temperature overnight, in which the molar ratio of TEOS : H_2O : H_3PO_4 was 1 : 11 : 0.02. Next, certain amounts of carbon nanospheres were added to 1 g of silica gel, and the mixture was sonicated for 30 min to obtain a homogeneous solution. Finally, this silica gel containing carbon nanospheres was mixed with 1 g of PVA solution and stirred for 6 h to obtain the precursor solution for electrospinning. For electrospinning process, the precursor solution was loaded into a plastic syringe and extruded through a needle equipped on the syringe at a feeding speed of 10 μL/min. Electrospinning was performed at an applied potential of 12 kV and a distance of 15 cm between the needle and the negative foil collector. The collected fibrous membrane (PVA/SiO_2/C) was dried at 80°C overnight and then calcined at 800°C for 2 h with heating rate of 4°C/min in air. The porous fibrous membranes obtained with carbon sphere concentrations of 20, 50, and 75 mg/mL were denoted as SiO_2NF-20, SiO_2NF-50, and SiO_2NF-75, respectively.

2.3. Characterization. Morphology of fibrous membranes was observed by scanning electron microscopy (SEM, Hitachi 4800) and transmission electron microscopy (TEM, Tecnai-G2-F30). X-ray diffraction (XRD) measurements were performed on a Shimadzu D6000. Attenuated total reflection Fourier transform infrared spectroscopy (ATR-FTIR) spectra were recorded using Bruker tensor II spectrometer within the wavenumber range of 4000–400 cm^{-1}. X-ray photoelectron spectroscopy (XPS) was performed with a PHI-5702 X-ray photoelectron spectrometer. Thermogravimetric analysis (TGA) was obtained at the heating rate of 10°C/min in air by the 1090B TGA instrument (DuPont Inc.).

3. Results and Discussion

The procedure for fabricating porous SiO_2 nanofibrous membrane is illustrated in Figure 1. Electrospinning was used to prepare carbon nanosphere incorporated electrospun fibers (PVA/SiO_2/C), which were then calcined at high temperature for the generation of porous SiO_2 nanofibers. Herein, carbon nanospheres were chosen to serve as templates to generate nanopores inside the SiO_2 nanofibers for two reasons. First, carbon nanospheres are readily decomposed together with PVA polymers in one step, as well as the SiO_2 condensation during the high temperature treatment. Besides, the surface of the carbon nanospheres synthesized by hydrothermal method has numerous polar terminal moieties, such as hydroxyl (-OH) and carboxylic acid (-COOH), which facilitate the dispersion of carbon nanospheres in the hydrophilic electrospinning solution [23].

Figure 2 presents the representative SEM images of carbon spheres, PVA/SiO_2/C fibers formed with various carbon nanosphere concentrations of 0, 50, and 75 mg/mL, respectively. The carbon nanospheres used for the electrospinning were synthesized by hydrothermal method and had an average diameter in the range of 90–130 nm (Figure 2(a)). As seen in Figure 2(b), the random nanofiber surface without carbon nanospheres is smooth and uniform with an average

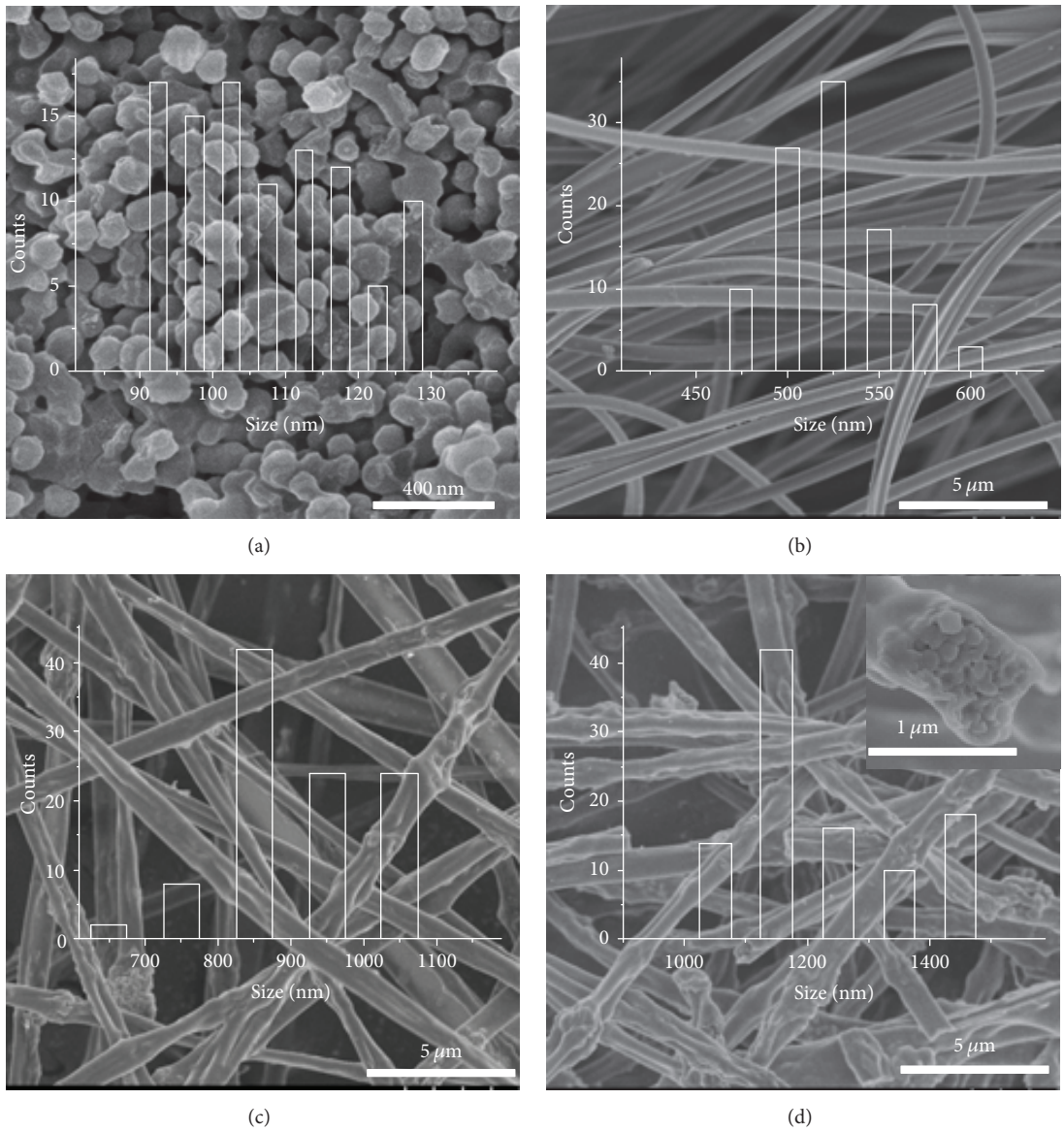

FIGURE 2: SEM images of the carbon spheres (a), PVA/SiO_2/C nanofibers with different concentrations of carbon nanospheres: 0 (b), 50 (c), and 75 mg/mL (d); inset of (d) is the cross section SEM image of fibers in (d); the inset graphs are the diameter distribution.

diameter of 530 nm. When 50 mg/mL of carbon nanospheres is introduced into the precursor solution, certain protuberances are observed on the fiber surface and the fiber diameter is in the wide range of 0.8~1.1 μm (Figure 2(c)). Compared with fibers in Figure 2(b), the increase of the diameter may be attributed to the higher viscosity of the electrospinning solution, which is caused by the interaction between carbon nanospheres and the PVA and hydrolyzed silica gel in the electrospinning solution. At a carbon nanosphere concentration of 75 mg/mL, the diameter of nanofibers increases to above 1.1 μm, and the protuberances on the fibers are more obvious perhaps due to the aggregation of nanospheres at a high concentration (Figure 2(d)). Inset of Figure 2(d) is a magnified SEM micrograph of the fiber cross section in Figure 2(d). It can be clearly seen that the carbon nanospheres are wrapped in the polymer shell other than on the fiber's exterior surface, which is attributed to the effect of solution surface tension [24]. The results in Figure 2 suggest that the carbon nanospheres can be easily encapsulated in the silica and PVA shell to form uniform core-shell structure nanofibers.

The disappearance of the organic PVA and occurrence of inorganic SiO_2 nanofibers after the calcination were evidenced by ATR-FTIR. Figure 3(a) shows the FTIR spectrum of the as-spun PVA/SiO_2/C nanofibers. It can be seen that there is a wide absorption band at 3350 cm^{-1}, which is assigned to the hydrogen bonded or H-O stretching vibration in water. The broad peak at 2938 cm^{-1} corresponds to the C-H stretching vibration and the in-plane bending vibration in -CH_2- [25]. The absorption features of carbon nanospheres

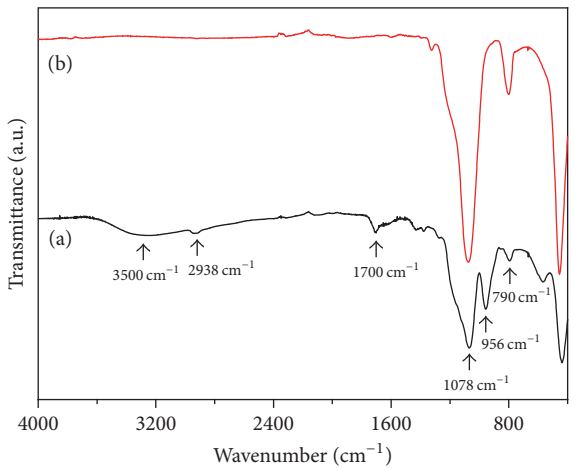

Figure 3: ATR-FTIR plots of PVA/SiO_2/C (a) and calcined SiO_2 membranes (b).

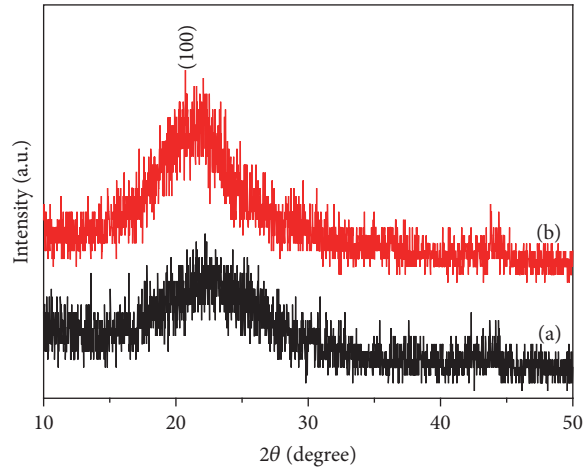

Figure 4: XRD plots of PVA/SiO_2/C (a) and calcined SiO_2 fiber membranes (b).

are found at 1700 cm^{-1}, which is attributed to the stretching vibration of C=O [23]. Besides, absorption peak at 956 cm^{-1} is assigned to the Si-OH bond. The peaks at 1078 cm^{-1} and 790 cm^{-1} are observed in the case of the Si-O-Si bond, which indicates that TEOS has been partially hydrolyzed to silicic acid and SiO_2 during the preparation of electrospun fibers. FTIR spectrum of silica fibrous membrane after calcination at 800°C for 2 h is exhibited in Figure 3(b). Compared with the plot of Figure 3(a), the peaks at 3350 cm^{-1}, 2938 cm^{-1}, and 1700 cm^{-1} disappeared, indicating that the PVA and carbon nanospheres have been completely decomposed. Meanwhile, the disappearance of Si-OH band at 956 cm^{-1} reveals the existence of silica by further polycondensation after high temperature calcination. In addition, the peaks at 1078 cm^{-1} and 790 cm^{-1} are significantly enhanced, which is attributed to the formation of inorganic silica fibers mainly containing Si-O-Si. As a result, the calcination process has removed organic polymer and carbon particles completely and left the inorganic SiO_2 fibers only.

To clarify the influence of the calcination on the crystalline phase, XRD patterns from 10° to 50° of PVA/SiO_2/C and calcined SiO_2 fibrous membranes are displayed in Figure 4. The broad diffraction peak around 21.5° suggests the nanofibers are in amorphous phase of silica, which can be indexed to the (100) lattice plane of the tridymite (JCPDS number 75-0638) (Figure 4(a)) [26]. No other obvious diffraction peak illustrates that the incorporated carbon spheres synthesized by the hydrothermal method are in amorphous phase. The diffraction peak is not significantly enhanced after calcination because of an amorphous phase of the silica and the porous structure of the fiber membrane resulting in a weak signal (Figure 4(b)).

Thermogravimetric analysis (TGA) was performed to understand the thermal behavior of as-spun fibers. Figure 5 shows the TGA spectra from 100 to 800°C of PVA, carbon spheres, and electrospun fibers without carbon nanosphere addition (PVA/SiO_2) and PVA/SiO_2/C samples. It is noted that the weight losses are near 100% for the PVA and carbon

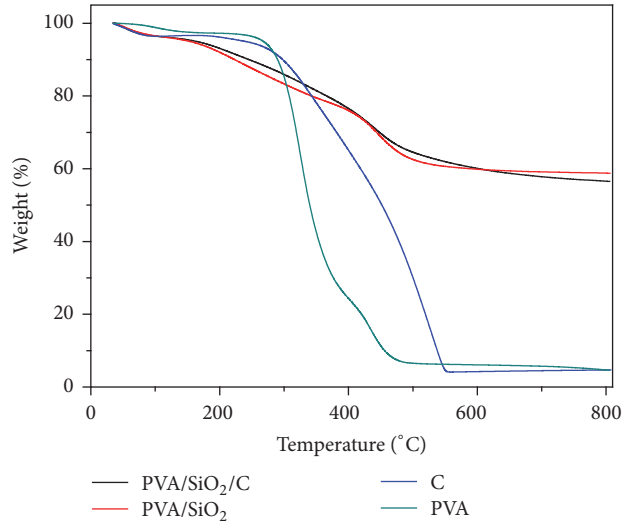

Figure 5: TGA plots of PVA/SiO_2 (a) and PVA/SiO_2/C (b) fibers.

spheres before 500°C and 550°C, respectively, indicating that they can be decomposed completely by the calcination temperature of 800°C used in this work. Weight loss around 100~250°C resulted from the moisture desorption [26]. The PVA is decomposed in a two-step process: dehydration of the polymer side chains at 250~350°C and C-C bond cleavage of the polymer chain from 400 to 500°C. The decomposition of carbon nanospheres was accomplished at 350~550°C [26]. Both as-spun PVA/SiO_2 and PVA/SiO_2/C fibers have similar weight loss tendencies that mainly occurred in the low temperature region. Incorporation of carbon nanospheres has no obvious influence on the total weight loss (44%) of the fiber membranes, which is due to the small weight ratio of the carbon spheres in the electrospinning solution. Furthermore, a slightly slower weight loss of the PVA/SiO_2/C fibers compared to PVA/SiO_2 fibers might be attributed to the interaction between carbon nanospheres and polymer chain.

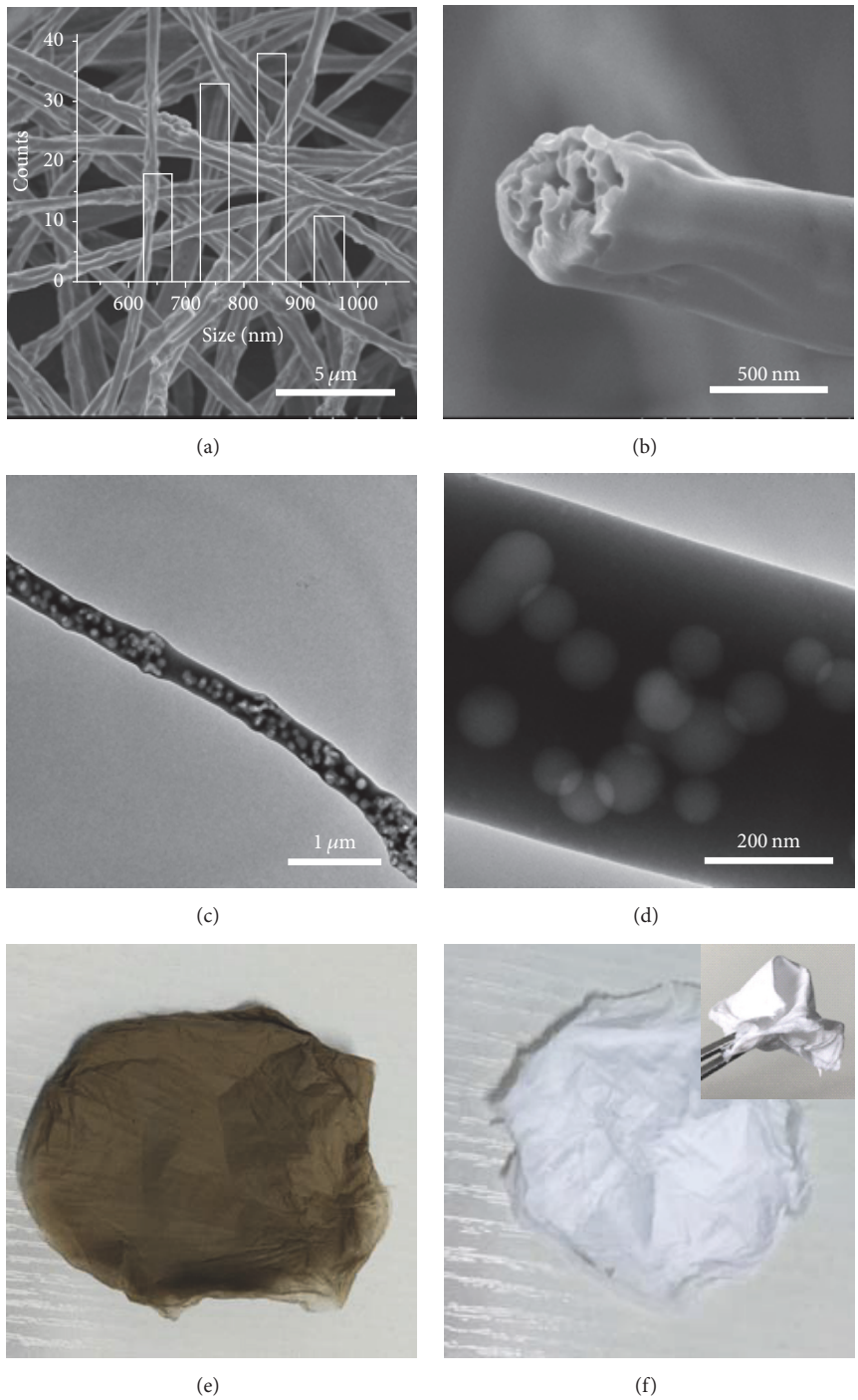

Figure 6: SEM ((a), (b)) and TEM ((c), (d)) images of the porous SiO_2 nanofibers; optical images of the PVA/SiO_2/C (e) and porous SiO_2 fibers (f); inset of (a) is the size distribution of the porous SiO_2 nanofibers.

No obvious weight loss of the porous SiO_2 fibers at high temperature shows their thermal stability, which means that the porous SiO_2 fibers can be easily recycled by calcination avoiding secondary pollution.

To investigate the morphology and size of nanofibers after calcination, the porous SiO_2 nanofibers by calcination of PVA/SiO_2/C fibers electrospun from a precursor solution with carbon sphere concentration of 50 mg/mL were examined by SEM and TEM measurements. From the SEM photographs and diameter distribution in Figure 6(a), it can be noted that the fiber diameter of the randomly oriented fibers is in the range of 0.7–0.9 μm, which is slightly smaller

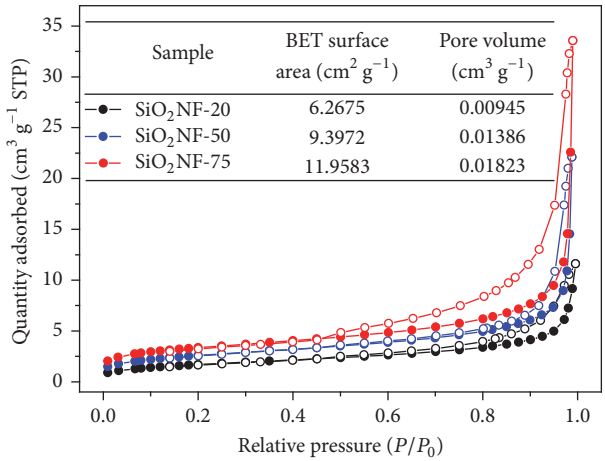

Figure 7: Nitrogen physisorption isotherms of SiO_2NF-20, SiO_2NF-50, and SiO_2NF-75 fibrous membranes. The "solid circles" and "empty circles" represent the adsorption and desorption curve, respectively.

than the diameter of the PVA/SiO_2/C fibers due to the removal of polymer and further polycondensation of the silica by calcination. Apparent nanopores can be observed in the cross section image of the fibers (Figure 6(b)), indicating that carbon nanospheres are removed and nanoporous SiO_2 fibers are obtained after calcinations. The average size of the nanopores is 70 nm smaller than the diameter of the carbon nanosphere templates, revealing that the oxidation of carbon and shrinkage of nanofibers were carried out simultaneously. Additionally, a few connected pores were produced because of the aggregation of carbon nanospheres. Figures 6(c) and 6(d) show the further investigation of the nanoporous SiO_2 fibers by TEM characterization. Due to the density difference, the nanopore structures can be observed inside the fiber with lighter color compared with SiO_2 fiber component with deeper color. Besides, the round shape nanopores uniformly and independently are distributed throughout the fiber, suggesting that the carbon nanoparticles were uniformly distributed inside the SiO_2 nanofibers during the electrospinning process. Moreover, all the nanopores are included inside the nanofibers other than opening pores, which is accordant with SEM results in Figure 2(d).

The electrospinning and subsequent calcination process were also accompanied with a color change of the fibrous membrane from brown (Figure 6(e)) to white (Figure 6(f)), due to the incorporation of carbon nanoparticles in the PVA/SiO_2/C fibers and removal of the carbon nanospheres of the porous SiO_2 fiber. More importantly, no obvious break was observed when the porous SiO_2 fiber membrane was folded and curled, as shown by the inset optical graphs in Figure 6(f), which suggests that the porous SiO_2 fiber membrane still maintains its flexibility after calcination like the pure SiO_2 fiber mats. These results in Figure 6 demonstrate that porous SiO_2 nanofibers with uniform internal nanoporous can be fabricated after one-step calcination of the electrospun nanofibers encapsulated with carbon nanosphere template.

To further investigate the influence of the added carbon spheres on the porous nanostructures, N_2 adsorption–desorption isotherms at 77 K SiO_2NF-20, SiO_2NF-20, and SiO_2NF-75 fiber membranes were carried out. The curves in Figure 7 illustrate type IV with a hysteresis loop, revealing characteristics of mesopores within the porous SiO_2 fiber mats [26]. The inset of Figure 7 displays the BET surface areas and pore volumes of the different porous fibrous membranes, which are ranked in the order of SiO_2NF-20 < SiO_2NF-20 < SiO_2NF-75. Notably, the more incorporated the carbon spheres are, the larger the BET surface areas and pore volumes are. These results suggested that the BET surface area and the pore volume of the porous membrance could be adjusted by turning the quantities of the carbon spheres.

The typical high resolution XPS spectra were acquired to further investigate the surface composition and chemical state of porous SiO_2 nanofibers. The XPS spectrum of Si2p region is displayed in Figure 8(a) with the characteristic peak at the binding energy of 103.7 eV corresponding to Si2p, indicating the state of Si^{4+} in porous SiO_2 nanofibers [27]. The peak located at binding energy of 532.8 eV can be assigned to the O^{2-} in the porous SiO_2 nanofibers (Figure 8(b)). The XPS results demonstrate the formation of SiO_2 after calcination of PVA/SiO_2/C, which is in good accordance with the results of XRD analysis.

4. Conclusions

We proposed a simple method for the rapid preparation of porous inorganic SiO_2 nanofibrous membrane with carbon nanospheres as templates. By treating PVA/SiO_2/C electrospun nanofibers at high temperature, carbon nanosphere template was removed and porous SiO_2 nanofibers were produced in one step. The obtained porous SiO_2 nanofibrous membrane shows high thermal stability and flexibility with uniform nanopores inside the fibers. BET surface area and the pore volume of the porous membrance could be controlled by turning the quantities of the carbon spheres. As calcination is a basic process in the preparation of inorganic nanofibers

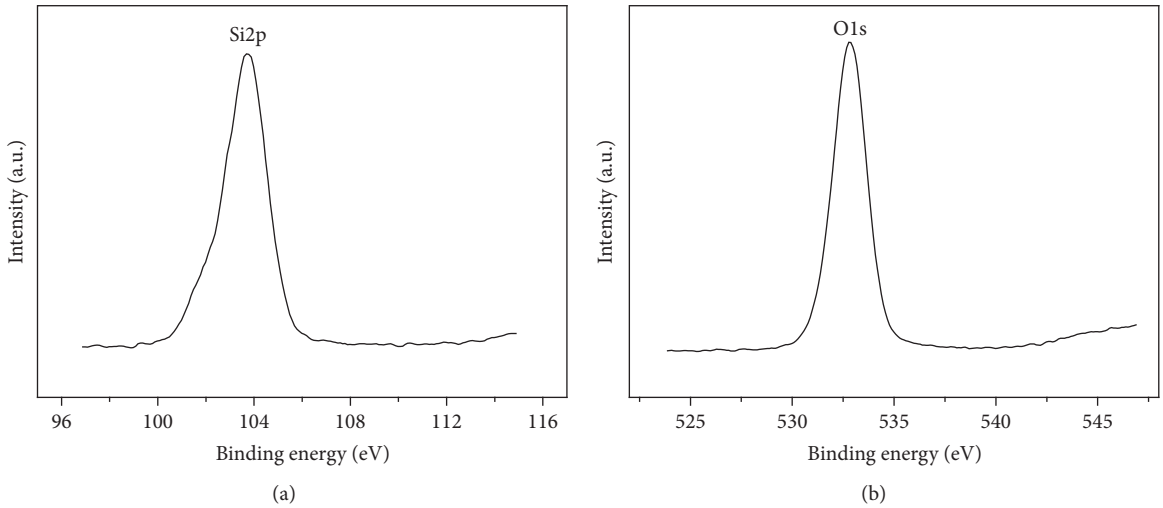

Figure 8: XPS spectra of porous SiO_2 nanofibers: (a) Si2p; (b) O1s.

by electrospinning and the carbon nanospheres have high chemical stability and surface compatibility, therefore the method can also be applied to the preparation of other porous inorganic nanofibers for practical application.

Conflicts of Interest

The authors declare that there are no conflicts of interest.

Acknowledgments

This work was supported by the National Natural Science Foundation of China (21501140, 21403165, and 51372197), the Science and Technology Department of Shaanxi Province (2015JQ2047 and 2016JQ2002), and the Key Innovation Team of Shaanxi Province (2014KCT-04).

References

[1] C. Niu, J. Meng, X. Wang et al., "General synthesis of complex nanotubes by gradient electrospinning and controlled pyrolysis," *Nature Communications*, vol. 6, article 7402, pp. 1–9, 2015.

[2] Z. Li, J. T. Zhang, Y. M. Chen, J. Li, and X. W. Lou, "Pie-like electrode design for high-energy density lithium-sulfur batteries," *Nature Communications*, vol. 6, article 8850, 2015.

[3] B. M. Baker, B. Trappmann, W. Y. Wang et al., "Cell-mediated fibre recruitment drives extracellular matrix mechanosensing in engineered fibrillar microenvironments," *Nature Materials*, vol. 14, no. 12, pp. 1262–1268, 2015.

[4] S. Wang, B. Y. Guan, L. Yu, and X. W. Lou, "Rational design of three-layered TiO_2@carbon@MoS_2 hierarchical nanotubes for enhanced lithium storage," *Advanced Materials*, vol. 29, no. 37, 2017.

[5] M. Chang, H. Wang, H. Li, J. Liu, and H. Du, "Facile preparation of novel Fe_2O_3/BiOI hybrid nanostructures for efficient visible light photocatalysis," *Journal of Materials Science*, vol. 53, no. 5, pp. 3682–3691, 2018.

[6] L. Wang, Y. Zhao, Y. Tian, and L. Jiang, "A general strategy for the separation of immiscible organic liquids by manipulating the surface tensions of nanofibrous membranes," *Angewandte Chemie International Edition*, vol. 54, no. 49, pp. 14732–14737, 2016.

[7] X. Zhao, Y. Li, T. Hua et al., "Low-resistance dual-purpose air filter releasing negative Ions and effectively capturing PM2.5," *ACS Applied Materials & Interfaces*, vol. 9, no. 13, pp. 12054–12063, 2017.

[8] C. Liu, P.-C. Hsu, H. Lee et al., "Transparent air filter for high-efficiency PM2.5 capture," *Nature Communications*, vol. 6, no. 6205, 2015.

[9] B. Khalid, X. Bai, H. Wei, Y. Huang, H. Wu, and Y. Cui, "Direct blow-spinning of nanofibers on a window screen for highly efficient PM2.5 removal," *Nano Letters*, vol. 17, no. 2, pp. 1140–1148, 2017.

[10] Q. Wen, J. Di, Y. Zhao, Y. Wang, L. Jiang, and J. Yu, "Flexible inorganic nanofibrous membranes with hierarchical porosity for efficient water purification," *Chemical Science*, vol. 4, no. 12, pp. 4378–4382, 2013.

[11] M. H. Müser and D. Shakhvorostov, "Why thick can be slick," *Science*, vol. 328, no. 5974, pp. 52-53, 2010.

[12] T. F. Jaramillo, K. P. Jørgensen, J. Bonde, J. H. Nielsen, S. Horch, and I. Chorkendorff, "Identification of active edge sites for electrochemical H_2 evolution from MoS_2 nanocatalysts," *Science*, vol. 317, no. 5834, pp. 100–102, 2007.

[13] K. S. Novoselov, D. Jiang, F. Schedin et al., "Two-dimensional atomic crystals," *Proceedings of the National Acadamy of Sciences of the United States of America*, vol. 102, no. 30, pp. 10451–10453, 2005.

[14] C. Yang, J. Lan, W. Liu, Y. Liu, Y. Yu, and X. Yang, "High-performance Li-Ion capacitor based on an activated carbon cathode and well-dispersed ultrafine TiO_2," *ACS Applied Materials & Interfaces*, vol. 9, no. 22, pp. 18710–18719, 2017.

[15] J. Wu, N. Wang, L. Wang, H. Dong, Y. Zhao, and L. Jiang, "Electrospun porous structure fibrous film with high oil adsorption capacity," *ACS Applied Materials & Interfaces*, vol. 4, no. 6, pp. 3207–3212, 2012.

[16] J. T. McCann, D. Li, and Y. Xia, "Electrospinning of nanofibers with core-sheath, hollow, or porous structures," *Journal of Materials Chemistry*, vol. 15, no. 7, pp. 735–738, 2005.

[17] S. Lee, K. Lee, G. D. Moon et al., "Preparation of macroporous carbon nanofibers with macroscopic openings in the surfaces and their applications," *Nanotechnology*, vol. 20, no. 44, Article ID 445702, 2009.

[18] J. Liu, M.-J. Chang, and H.-L. Du, "Facile preparation of cross-linked porous poly(vinyl alcohol) nanofibers by electrospinning," *Materials Letters*, vol. 183, pp. 318–321, 2016.

[19] J. Liu, M.-J. Chang, and H.-L. Du, "Fabrication and photocatalytic properties of flexible BiOI/SiO_2 hybrid membrane by electrospinning method," *Journal of Nanoscience and Nanotechnology*, vol. 17, no. 6, pp. 3792–3797, 2017.

[20] H. Shan, X. Wang, F. Shi, J. Yan, J. Yu, and B. Ding, "Hierarchical porous structured SiO_2/SnO_2 nanofibrous membrane with super flexibility for molecular filtration," *ACS Applied Materials & Interfaces*, vol. 9, no. 22, pp. 18966–18976, 2017.

[21] X. H. Li, C. L. Shao, and Y. C. Liu, "A simple method for controllable preparation of polymer nanotubes via a single capillary electrospinning," *Langmuir*, vol. 23, no. 22, pp. 10920–10923, 2007.

[22] W. Wang, J. Zhou, S. Zhang et al., "A novel method to fabricate silica nanotubes based on phase separation effect," *Journal of Materials Chemistry*, vol. 20, no. 41, pp. 9068–9072, 2010.

[23] X. Sun and Y. Li, "Colloidal carbon spheres and their core/shell structures with noble-metal nanoparticles," *Angewandte Chemie*, vol. 43, no. 5, pp. 597–601, 2004.

[24] J. Liu, J. Shi, L. Jiang et al., "Segmented magnetic nanofibers for single cell manipulation," *Applied Surface Science*, vol. 258, no. 19, pp. 7530–7535, 2012.

[25] L. Wu, X. Yuan, and J. Sheng, "Immobilization of cellulase in nanofibrous PVA membranes by electrospinning," *Journal of Membrane Science*, vol. 250, no. 1-2, pp. 167–173, 2005.

[26] X. Mao, Y. Si, Y. Chen et al., "Silica nanofibrous membranes with robust flexibility and thermal stability for high-efficiency fine particulate filtration," *RSC Advances*, vol. 2, no. 32, pp. 12216–12223, 2012.

[27] M. Wang, X. Li, W. Hua, L. Shen, X. Yu, and X. Wang, "Electrospun Poly(acrylic acid)/Silica hydrogel nanofibers Scaffold for highly efficient adsorption of lanthanide Ions and its photoluminescence performance," *ACS Applied Materials & Interfaces*, vol. 8, no. 36, pp. 23995–24007, 2016.